Optical Anisotropy and Photopumped Lasing near 250 nm from Semipolar $(1\bar{1}02)$ $Al_xGa_{1-x}N$/AlN Quantum Wells with Cleaved Mirrors

Shuhei Ichikawa,[†] Mitsuru Funato, and Yoichi Kawakami[*]
Department of Electronic Science and Engineering, Kyoto University, Kyoto 615-8510, Japan

(Received 18 August 2022; accepted 8 September 2022; published 3 October 2022)

The optical anisotropy of *r*-plane $Al_xGa_{1-x}N$/AlN quantum wells (QWs) is investigated theoretically and experimentally. Theoretical calculations predict that as the Al composition is increased from 0 to 1, the in-plane polarization switches from $\mathbf{E} \perp [11\bar{2}0]$ to $\mathbf{E} \perp [1\bar{1}01]$ at an Al composition of approximately 0.2. The polarization properties are nearly independent of the well width, particularly when the well width is thicker than approximately 1.5 nm. Photoluminescence spectroscopy of the fabricated *r*-plane $Al_xGa_{1-x}N$/AlN QWs experimentally confirms the theoretical prediction. The $\mathbf{E} \perp [1\bar{1}01]$ polarization enables the emitted light to propagate along the $[11\bar{2}0]$ direction. Using this property, photopumped lasing at approximately 250-nm wavelength at 11 K is demonstrated from an *r*-plane $Al_xGa_{1-x}N$/AlN QW with the cleaved $(11\bar{2}0)$ *a* planes as cavity mirrors.

DOI: 10.1103/PhysRevApplied.18.044005

I. INTRODUCTION

$Al_xGa_{1-x}N$-based laser diodes and light-emitting diodes are promising alternatives to current gas-based deep UV (DUV) light sources due to their compactness and harmlessness. Such devices have been extensively studied and show steady progress [1–14]. Recently, electrically driven laser diodes emitting in the UV-C [12,14] or UV-B [13] spectral regions have been demonstrated. Semipolar or nonpolar planes have the potential to further improve device performance because compared with light emitters on the conventional (0001) plane, they involve weaker spontaneous and piezoelectric polarizations along the growth direction [15]. It has experimentally been confirmed that due to the reduced polarization effect, $Al_xGa_{1-x}N$-based quantum wells (QWs) on $(1\bar{1}02)$ semipolar *r*-plane AlN substrates show enhanced radiative recombination in the DUV spectral region [16].

A characteristic feature of semipolar and nonpolar $Al_xGa_{1-x}N$-based QWs is the optical anisotropy caused by the valence-band structures. In wurtzite semiconductors such as AlN and GaN, spin-orbit interactions and noncubic crystal fields cause the valence-band maxima to split near the Γ point in the Brillouin zone. Typically, there are three types of valence bands: heavy-hole (HH), light-hole (LH), and crystal-field split-off-hole (CH) bands. The topmost valence band in AlN is the CH band, governed by the p_z-like state [17–22], whereas that in GaN is the HH band, governed by p_x- and p_y-like states [23–25]. Here, the *z* axis corresponds to the *c* axis in wurtzite structures and the *x* and *y* axes are in the *c* plane. Consequently, the emission from AlN is predominantly polarized parallel to the *c* axis ($\mathbf{E} \parallel c$), whereas that from GaN is polarized perpendicular to the *c* axis ($\mathbf{E} \perp c$), where **E** is the electric field vector of emitted light. Additionally, strain and quantum confinement play crucial roles in determining the valence-band order in QWs due to the quantum confinement Stark effect and the different effective mass of each valence band [26]. The optical anisotropy in $Al_xGa_{1-x}N$ QWs on the *c* or nonpolar plane is well studied [26–30] and the experimental results are reasonably backed by theoretical considerations.

By contrast, the number of experimental studies on semipolar $Al_xGa_{1-x}N$ films and QWs is limited [16,31–35]. One reason is related to the substrate. Because AlN substrates are expensive, most studies use foreign substrates such as sapphire and ZnO [31–33,35]. These substrates induce numerous threading dislocations. In addition, the growth conditions completely differ from the *c*-plane growth. Even in homoepitaxy-based growth, nonpolar $Al_xGa_{1-x}N$ QWs tend to be wavy [29,30] and semipolar AlN shows numerous growth pits [36].

We have recently established the homoepitaxy-based growth conditions for $(1\bar{1}02)$ *r*-plane $Al_xGa_{1-x}N$ QWs with atomically smooth surfaces [36] and high optical qualities [16]. This study aims at theoretically and experimentally revealing the optical anisotropy in $Al_xGa_{1-x}N$/AlN QWs on *r*-plane AlN substrates. Theoretically, the $\mathbf{k} \cdot \mathbf{p}$ perturbation theory is adopted, while

[*]kawakami@kuee.kyoto-u.ac.jp
[†]Present address: Division of Electrical, Electronic and Infocommunications Engineering, Osaka University, Suita, Osaka 565-0871, Japan.

experimentally, the in-plane polarization properties of the high-quality $Al_xGa_{1-x}N$/AlN QWs grown on the *r*-plane AlN substrates are investigated by photoluminescence (PL) spectroscopy. Both the theory and experiments consistently show the dominant optical polarization along the $[1\bar{1}01]$ direction for Al compositions greater than approximately 0.2. One potential application of this polarization property is to form laser cavities via cleavage at the $\{11\bar{2}0\}$ planes. We demonstrate photopumped lasing at 11 K from $Al_xGa_{1-x}N$/AlN QWs on *r*-plane AlN substrates with cleaved mirror cavities.

II. THEORETICAL PREDICTIONS OF THE OPTICAL ANISOTROPY

We perform theoretical calculations based on the $\mathbf{k}\cdot\mathbf{p}$ perturbation theory [15]. The material parameters are from Ref. [37] except for the deformation potentials, which are from our recent proposals [22,25]. The evaluated bandgap difference between the unstrained AlN barrier and strained $Al_xGa_{1-x}N$ well is divided into the band offsets at the conduction and valence bands with a ratio of 7:3, respectively. Although the deformation potentials for the conduction bands are not given in Refs. [22,25], this assumption for the band-offset ratio (7:3) allows the band structures to be calculated only using the exciton deformation potentials. (The excitonic effect is not included in the transition-energy calculations.)

Figure 1 schematically illustrates the wurtzite crystal structure and the $(1\bar{1}02)$ *r* plane. There are two important in-plane directions: $[1\bar{1}01]$ and $[11\bar{2}0]$. The $[1\bar{1}01]$ direction is parallel to the projection of the *c* axis on the *r* plane (c^*), while the $[11\bar{2}0]$ direction is perpendicular to the *c* axis. The in-plane polarization degree $\rho_{\rm in}$ is defined as

$$\rho_{\rm in} = \frac{I_{\mathbf{E}\perp c^*} - I_{\mathbf{E}\|c^*}}{I_{\mathbf{E}\perp c^*} + I_{\mathbf{E}\|c^*}}. \quad (1)$$

Figure 2 shows the calculated in-plane polarization degree of *r*-plane $Al_xGa_{1-x}N$/AlN QWs as functions of the well width and the Al composition. The polarization

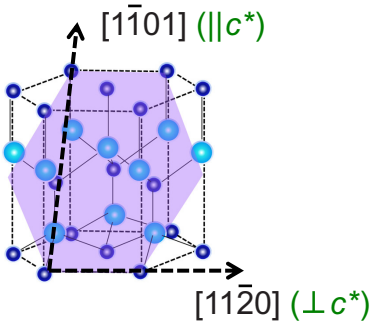

FIG. 1. A schematic of the wurtzite structure with the *r* plane and two important crystal directions.

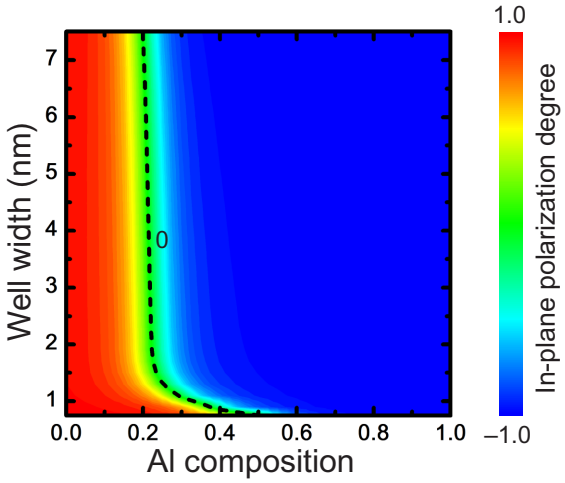

FIG. 2. The calculated in-plane polarization degree of *r*-plane $Al_xGa_{1-x}N$/AlN QWs as functions of the well width and the Al composition.

switches from $\mathbf{E}\perp c$ ($\rho_{\rm in} > 0$) to $\mathbf{E}\parallel c^*$ ($\rho_{\rm in} < 0$) at an Al composition of approximately 0.2. The switching is nearly independent of the well width when the well width is thicker than approximately 1.5 nm.

III. EXPERIMENTAL DETERMINATION OF THE OPTICAL ANISOTROPY

A. Experimental procedures

$Al_xGa_{1-x}N$/AlN QWs with various well widths and Al compositions are fabricated on semipolar *r*-plane AlN substrates by metalorganic vapor phase epitaxy (MOVPE) at 500 Torr, which is the optimized reactor pressure for semipolar-plane growth [36]. The 400-nm-thick AlN epitaxial layers are initially grown on the substrates and $Al_xGa_{1-x}N$/AlN QWs are subsequently fabricated. The well width varies but the barrier (including the cap layer) width is 16 nm. The well widths and Al compositions are estimated by x-ray diffraction measurements and transmission electron microscopy.

Two series of QWs are fabricated. One consists of *r*-plane $Al_{0.8}Ga_{0.2}N$/AlN QWs with various well widths (L_w) from 0.5 to 7.0 nm, and the other consists of *r*-plane approximately 1.5-nm-thick $Al_xGa_{1-x}N$/AlN QWs with various Al compositions. The variation of the in-plane polarization properties of the former and latter series of QWs correspond to those along the vertical and horizontal axes of Fig. 2.

The fabricated QWs are characterized by polarization PL measurements at 9.5 K using an ArF excimer laser (193 nm) as an excitation source. The typical excitation power density is a few MW/cm^2. The samples are excited at an angle of 60° from the surface normal and the PL signals are detected at the surface normal. A 50-cm monochromator

equipped with a liquid-N_2-cooled CCD camera (resolution 0.1 nm) is used for the detection. To investigate the in-plane polarization degree, a linear polarizer is placed within the optical path of the collimated PL. Because the PL signal after the polarizer is weak, the samples are excited by a relatively strong ArF laser.

B. In-plane polarization properties of *r*-plane $Al_{0.8}Ga_{0.2}N$/AlN QWs with different well widths

Figure 3(a) shows PL spectra of *r*-plane $Al_{0.8}Ga_{0.2}N$/AlN QWs with L_w of 1.4 and 7.0 nm at 9.5 K, where the polarization direction is either $\mathbf{E} \parallel c^*$ or $\mathbf{E} \perp c^*$. (The PL intensity is either maximum or minimum when $\mathbf{E} \parallel c^*$ or $\mathbf{E} \perp c^*$.) Both samples show strong polarization along the $\mathbf{E} \parallel c^*$. Furthermore, we examine five QWs with different well widths between 0.5 nm and 7.0 nm (but with nearly the same Al composition). Figure 3(b) shows the estimated polarization degrees. Although the experimental data show some scattering, the values are always negative ($\mathbf{E} \parallel c^*$) and nearly independent of the well widths. These trends are consistent with the theoretical calculation in Fig. 2, which is also shown as a blue curve in Fig. 3(b). (The inferior linear polarizability in the experiments compared to that in the theoretical calculations is likely due to experimental issues such as light scattering within the samples.)

C. In-plane polarization properties of *r*-plane approximately 1.5-nm-thick $Al_xGa_{1-x}N$/AlN QWs with various Al compositions

Figure 4(a) shows the estimated in-plane polarization degree of *r*-plane approximately 1.5-nm-thick $Al_xGa_{1-x}N$/AlN QWs as a function of the Al composition. The in-plane polarization degree is negative for Al compositions greater than approximately 0.2 (i.e., $\mathbf{E} \parallel c^*$). Although the thickness differs, the result for an *r*-plane GaN/AlN (approximately 0.4 nm = 2 molecular layers) is also plotted. (For this QW, the thickness is reduced to avoid lattice relaxation.) The GaN/AlN QW exhibits a positive in-plane polarization degree. The observed experimental

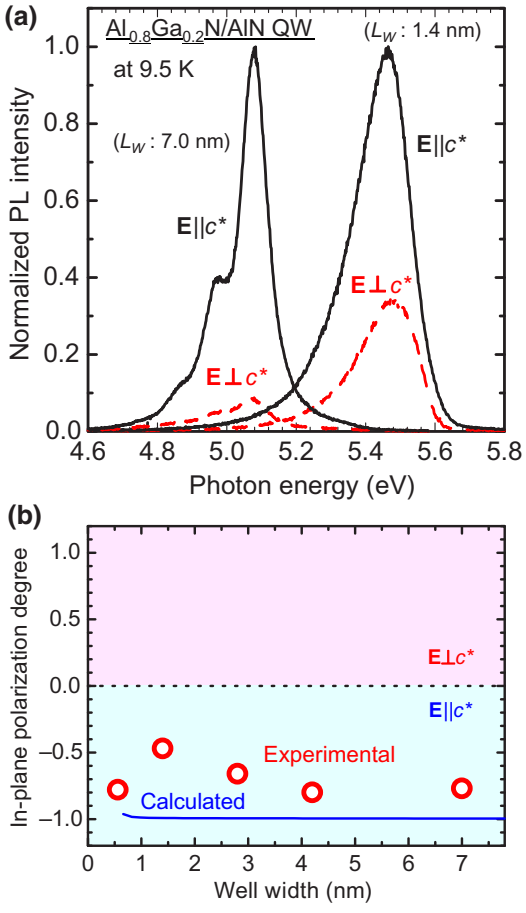

FIG. 3. (a) Polarization PL spectra of *r*-plane $Al_{0.8}Ga_{0.2}N$/AlN QWs at 9.5 K. Spectra for $\mathbf{E} \parallel c^*$ or $\mathbf{E} \perp c^*$ are shown. (b) In-plane polarization degrees estimated for $Al_{0.8}Ga_{0.2}N$/AlN QWs with various well widths. L_w denotes the well width.

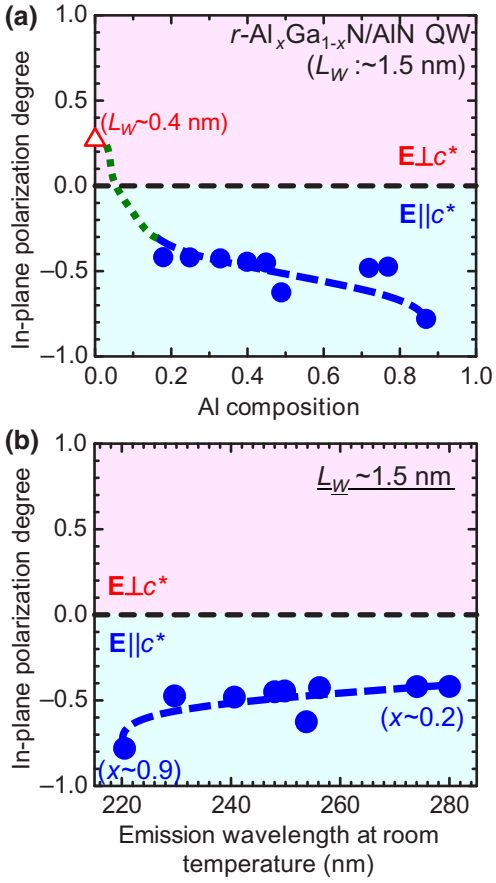

FIG. 4. (a) The Al composition dependence of the in-plane polarization degree of the *r*-plane $Al_xGa_{1-x}N$/AlN QWs with approximately 1.5-nm-thick well layers. To avoid lattice relaxation, the well width of the GaN/AlN QW is approximately 0.4 nm. (b) The emission-wavelength dependence of the in-plane polarization degree of the *r*-plane $Al_xGa_{1-x}N$/AlN QWs.

results, including the finding for the GaN/AlN QW, agree well with the calculation results shown in Fig. 2.

Figure 4(b) replots the results in Fig. 4(a) as a function of the emission wavelength at room temperature. The *r*-plane $Al_xGa_{1-x}N$/AlN QWs realize $\rho_{in} < 0$ over a wide DUV spectral range spanning from 220 nm to 280 nm.

Our theoretical calculation and experimental results consistently demonstrate that the in-plane polarization degrees of *r*-plane $Al_xGa_{1-x}N$/AlN QWs are negative for Al compositions greater than approximately 0.2 and nearly independent of the QW width. In particular, the negative in-plane polarization degree means polarization along the $[1\bar{1}01]$ direction ($\mathbf{E} \parallel c^*$) and enables us to fabricate the laser cavity by cleavage. The feasibility of this potential application is discussed in Sec. IV.

IV. PHOTOPUMPED LASING

For lasers, an optical cavity composed of a pair of cleaved mirrors is desirable because the atomically flat mirrors are aligned in parallel automatically and suppress the cavity loss. Thus, the optical polarization should be parallel to a cleaved plane. For *r*-plane QWs, because there are no cleavable planes perpendicular to the $[1\bar{1}01]$ direction, the optical polarization perpendicular to that direction ($\mathbf{E} \perp c^*$) is not preferable. On the other hand, when the optical polarization is parallel to the $[1\bar{1}01]$ direction ($\mathbf{E} \parallel c^*$, i.e., $\rho_{in} < 0$), the $(11\bar{2}0)$ *a* plane can be used as a cleaved mirror.

The theoretical and experimental investigations in the previous sections show that the optical polarization of *r*-plane $Al_xGa_{1-x}N$/AlN QWs is along the $[1\bar{1}01]$ direction ($\mathbf{E} \parallel c^*$) in wide ranges of the well width and Al composition. This is a preferential direction for laser cavities to form by cleavage. In this section, we first discuss an appropriate design of QW structures for highly efficient emitters and then demonstrate photopumped lasing from an *r*-plane $Al_xGa_{1-x}N$/AlN QW with a cleaved mirror cavity.

A. Structure design for higher emission efficiency

There are two common approaches to control the emission wavelength. One is to adjust the Al composition in the well layers. The other is to adjust the well width. However, their impacts on the optical properties differ completely. To show this, the squares of the overlap integrals of the electron and hole wavefunctions in *r*-plane $Al_xGa_{1-x}N$/AlN QWs are calculated. (It is noteworthy that our overlap calculations well reproduce the experimental results of time-resolved PL [16].) The calculated results (Fig. 5) indicate that controlling the wavelength using a constant well width (1.5 nm) with a variable Al composition results in an insignificant reduction in the overlap.

On the contrary, controlling the wavelength using a constant Al composition (80%) with a variable well width drastically decreases the overlap at longer wavelengths

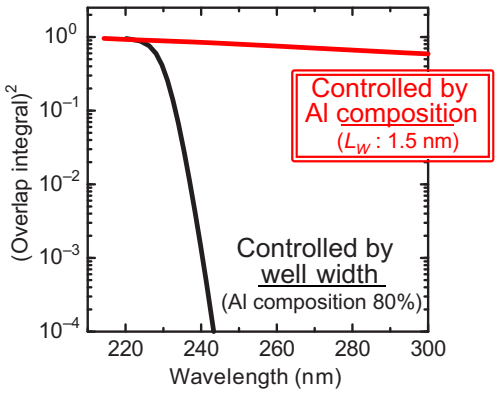

FIG. 5. The calculated squares of the overlap integrals of the electron and hole wavefunctions in *r*-plane $Al_xGa_{1-x}N$/AlN QWs as a function of the transition energy (wavelength). The wavelength is controlled through a constant well width (1.5 nm) with variable Al compositions or a constant Al composition (80%) with variable well widths.

(i.e., in wider wells). This is due to the polarization-induced internal electric fields. (Although the internal electric fields in *r*-plane QWs are much weaker than those in *c*-plane QWs, they are not zero unlike nonpolar-plane QWs [16].) Because the radiative recombination probability is proportional to the square of the overlap integral, the emission wavelengths of semipolar $Al_xGa_{1-x}N$/AlN QWs should be controlled by the Al compositions while maintaining a narrow well width (approximately 1.5 nm) for a high internal quantum efficiency (IQE).

We experimentally examine the predicted wavelength dependence of the radiative recombination probability (i.e., the emission intensity) of *r*-plane $Al_xGa_{1-x}N$/AlN QWs (Fig. 5). The standard QW is a 1.4-nm-thick $Al_{0.8}Ga_{0.2}N$/AlN QW and two other QWs with a different L_w or a different Al composition are compared.

These QWs are characterized by PL measurements using a Ti:Al_2O_3 fourth-harmonic-generation laser (approximately 210 nm) to selectively excite the well layers. This experimental setup realizes weak excitation conditions, avoiding the many-body effects and the screening effects of the internal electric fields. The detection of PL is ensured by a monochromator with a CCD camera.

Figure 6(a) shows the PL spectra of the *r*-plane $Al_{0.8}Ga_{0.2}N$/AlN ($L_w = 1.4$ or 4.2 nm) and $Al_{0.5}Ga_{0.5}N$/AlN ($L_w = 1.7$ nm) QWs at 6.5 K. Reduction of the Al compositions from 0.8 to 0.5 with a nearly constant well width of approximately 1.5 nm shifts the emission wavelengths from 224 nm to 250 nm. Moreover, widening of the well widths from 1.4 nm to 4.2 nm shifts the emission wavelengths of the $Al_{0.8}Ga_{0.2}N$/AlN QWs from 224 nm to 232 nm. Figure 6(b) shows the temperature dependencies of the integrated PL intensities of these QWs. The thermal quenching of the 1.7-nm-thick $Al_{0.5}Ga_{0.5}N$/AlN QW is almost the same as that of the

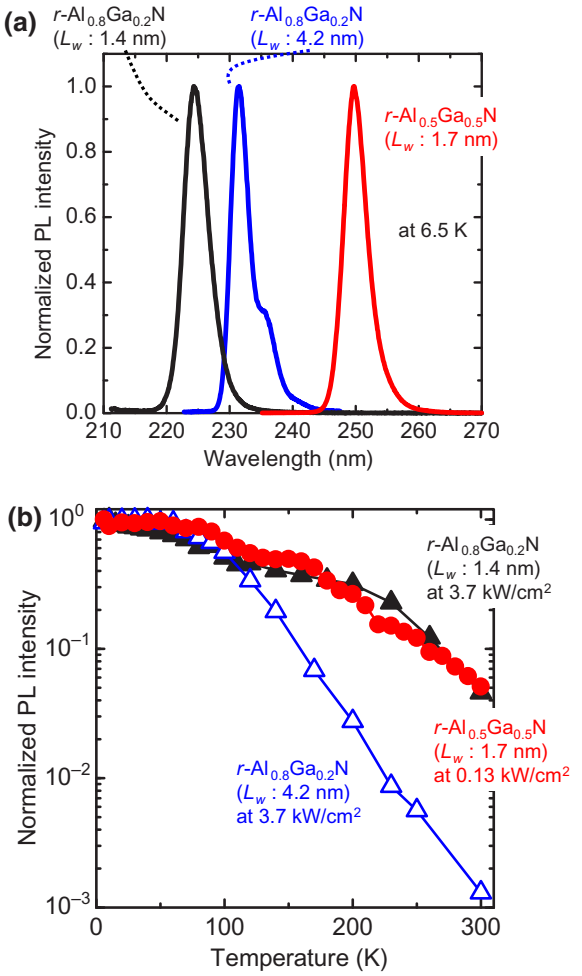

FIG. 6. (a) The PL spectra of the *r*-plane $Al_{0.8}Ga_{0.2}N$/AlN ($L_w = 1.4$ nm or 4.2 nm) and $Al_{0.5}Ga_{0.5}N$/AlN ($L_w = 1.7$ nm) QWs at 6.5 K. (b) The temperature dependencies of the integrated PL intensities for these QWs.

1.4-nm-thick $Al_{0.8}Ga_{0.2}N$/AlN QW despite the large difference in the emission wavelengths. On the other hand, the thermal quenching of the 4.2-nm-thick $Al_{0.8}Ga_{0.2}N$/AlN QW is much stronger than those of the other QWs with narrower well layers even though the emission wavelengths differ only slightly from the 1.4-nm-thick $Al_{0.8}Ga_{0.2}N$/AlN QW. This is because variations in the Al compositions have a negligible impact on the radiative recombination probability, whereas widening the well width drastically degrades the radiative recombination probability (Fig. 5). Thus, we experimentally confirm that wavelength control by varying Al compositions with a constant well width can effectively maintain a high IQE of semipolar $Al_xGa_{1-x}N$/AlN QWs with various emission wavelengths.

Figures 4–6 predict that *r*-plane $Al_xGa_{1-x}N$/AlN QWs with various Al compositions and a narrow well width (approximately 1.5 nm) can realize highly efficient lasers with cleaved mirrors in a spectral range of 220–280 nm.

B. Experimental results of photopumped lasing

Photopumping experiments are performed for an *r*-plane $Al_{0.5}Ga_{0.5}N$/AlN six-period QW structure (6QW) with 1.7-nm-thick well layers. The QW is designed for a 250-nm emission. The in-plane polarization degree of the QW is −0.63, indicating a strong polarization along $\mathbf{E} \parallel c^*$. This is similar to other $Al_xGa_{1-x}N$/AlN QWs examined in this study.

Figure 7 shows the experimental setup. The excitation source is an ArF excimer laser (193 nm) at a 25-Hz repetition rate with a pulse width of 4 ns. A Fabry-Perot cavity with a length of 2 mm forms along the $[11\bar{2}0]$ direction by cleavage. The fabricated sample is optically pumped from the surface by the ArF excimer laser at 11 K and the emissions from the *a*-plane facet are detected by a CCD camera through a monochromator. A high-reflection coating is not applied on the cleaved *a* planes.

Figure 8(a) shows the PL spectra of the *r*-plane $Al_{0.5}Ga_{0.5}N$/AlN 6QW with various excitation power densities. The peak wavelength is approximately 250 nm. Stimulated emission appears under strong excitation conditions. Figure 8(b) plots the excitation power dependencies of the PL intensity and line width. The emission intensity increases suddenly and the spectrum narrows above a threshold excitation power density of approximately 500 kW/cm^2. Hence, the stimulated emission is experimentally demonstrated from the semipolar-plane $Al_xGa_{1-x}N$ QW with cleaved mirrors.

We compare the obtained threshold power density with the reported values obtained at room temperature. A stimulated emission from an $Al_xGa_{1-x}N$ multiple QW fabricated on SiC at a wavelength in the sub-250-nm region has been reported [38]. It showed a threshold power density as high as 1.2 MW/cm^2. More recently, $Al_xGa_{1-x}N$-based photopumped lasers fabricated on sapphire [39–45] and *c*-plane AlN [46–54] substrates have been reported. Figure 9 summarizes the lasing-wavelength dependence of the reported threshold power densities. The reported threshold power densities are nearly independent of the substrate type

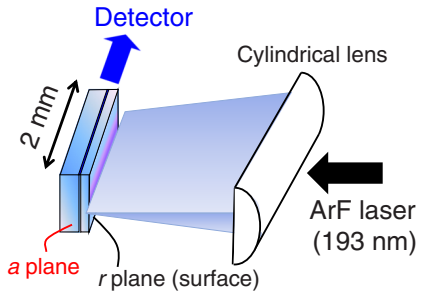

FIG. 7. A schematic of the photopumping measurement setup using an ArF excimer laser (193 nm) as an excitation source.

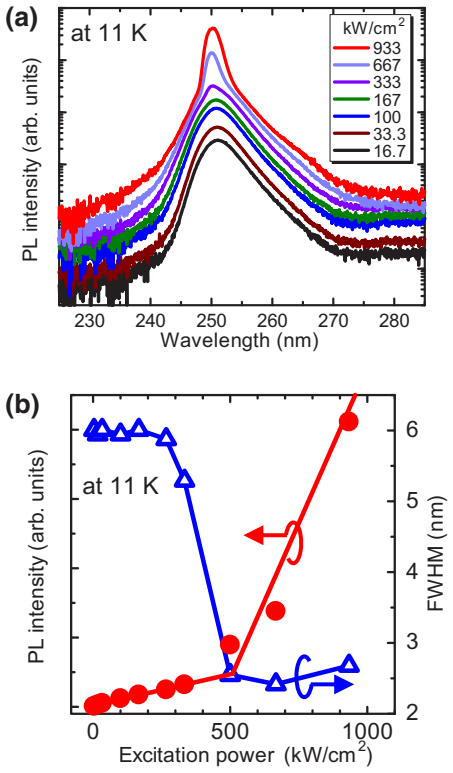

FIG. 8. (a) Spontaneous and stimulated emission spectra of the *r*-plane $Al_{0.5}Ga_{0.5}N$/AlN 6QW at 11 K. (b) The excitation power dependencies of the PL intensity and line width. FWHM, full width at half maximum.

despite the vastly different threading dislocation densities in the epilayers on sapphire and AlN, suggesting the presence of recombination channels other than threading dislocations.

Figure 9 plots the experimental result of the fabricated semipolar *r*-plane $Al_{0.5}Ga_{0.5}N$/AlN 6QW. Although this study realizes photopumped lasing at a cryogenic temperature, where the threshold power density can be lowered, the obtained value is not necessarily lower than previous reports, indicating that our sample can be improved. For example, our *r*-plane $Al_{0.5}Ga_{0.5}N$/AlN QW does not have optical-confinement structures. Hence, waveguiding using $Al_yGa_{1-y}N$ ($y > x$) should effectively reduce the threshold power density. Furthermore, the cleavability of the *a* plane should be considered. In $Al_xGa_{1-x}N$-based lasers fabricated on the *c* plane, the *m* planes are used as cleaved cavity mirrors. Because the *a* plane generally has a poorer cleavability than the *m* plane, our *r*-plane QW may have a larger mirror loss than a *c*-plane QW. High-reflection coatings such as dielectric multilayers on the *a*-plane facets may compensate for the mirror loss. Moreover, semipolar QWs with the off angles toward the $\langle 11\bar{2}0 \rangle$ directions such as $(11\bar{2}2)$ QWs are also attractive to suppress mirror loss because the *m* plane can be used as cavity mirrors.

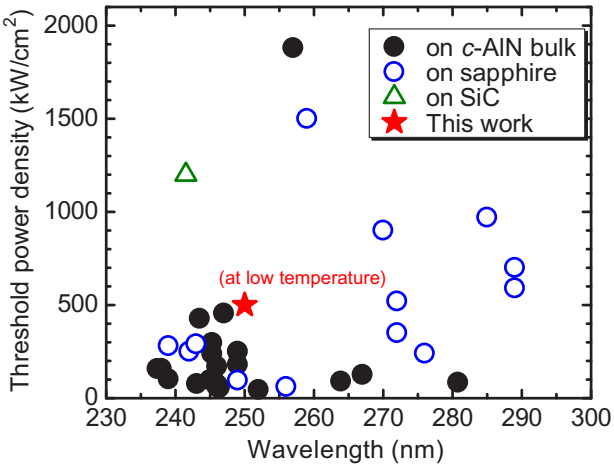

FIG. 9. The lasing-wavelength dependence of the reported threshold power densities for $Al_xGa_{1-x}N$ MQWs fabricated on SiC, [38] sapphire, [39–45] and *c*-plane AlN [46–54] substrates. Also plotted is the experimental result of the semipolar *r*-plane $Al_{0.5}Ga_{0.5}N$/AlN 6QW fabricated in this study. Our data are acquired at a low temperature (LT) of 11 K. Other data are obtained at room temperature.

V. SUMMARY

We investigate the optical anisotropy and photopumped lasing properties of $Al_xGa_{1-x}N$/AlN QWs grown on semipolar *r*-plane AlN substrates. Theoretical calculations predict that as the Al composition is increased from 0 to 1, the polarization switches from $\mathbf{E} \perp c$ ($\rho_{in} > 0$) to $\mathbf{E} \parallel c^*$ ($\rho_{in} < 0$) at an Al composition of approximately 0.2. In addition, the polarization is nearly independent of the well width. This prediction is experimentally confirmed for two series of *r*-plane $Al_xGa_{1-x}N$/AlN QWs with different well widths or different Al compositions. With the $\mathbf{E} \parallel c^*$ polarization, the emitted UV light can propagate along the $[11\bar{2}0]$ direction, enabling the formation of cavity mirrors with the nonpolar $\{11\bar{2}0\}$ cleaved facets. Photopumping by an ArF laser (193 nm) realizes lasing at an approximately 250 nm wavelength at 11 K with a threshold power density of 500 kW/cm^2 from an *r*-plane $Al_xGa_{1-x}N$/AlN QW with a cleaved mirror cavity.

ACKNOWLEDGMENTS

This work was partially supported by the Japan Society for the Promotion of Science (JSPS) KAKENHI (Grants No. JP20H05622 and No. JP21H04661). We would like to acknowledge JFE Mineral for supplying the AlN substrates.

[1] A. Khan, K. Balakrishnan, and T. Katona, Ultraviolet light-emitting diodes based on group three nitrides, Nat. Photon. **2**, 77 (2008).

[2] A. Fujioka, T. Misaki, T. Maruyama, Y. Narukawa, and T. Mukai, Improvement in output power of 280-nm deep ultraviolet light-emitting diode by using AlGaN multi quantum wells, Appl. Phys. Express **3**, 041001 (2010).

[3] C. Pernot, M. Kim, S. Fukahori, T. Inazu, T. Fujita, Y. Nagasawa, A. Hirano, M. Ippommatsu, M. Iwaya, S. Kamiyama, I. Akasaki, and H. Amano, Improved efficiency of 255–280 nm AlGaN-based light-emitting diodes, Appl. Phys. Express **3**, 061004 (2010).

[4] T. Oto, R. G. Banal, K. Kataoka, M. Funato, and Y. Kawakami, 100 mW deep-ultraviolet emission from aluminium-nitride-based quantum wells pumped by an electron beam, Nat. Photon. **4**, 767 (2010).

[5] M. Shatalov, W. Sun, R. Jain, A. Lunev, X. Hu, A. Dobrinsky, Y. Bilenko, J. Yang, G. A. Garrett, L. E. Rodak, M. Wraback, M. Shur, and R. Gaska, High power AlGaN ultraviolet light emitters, Semicond. Sci. Technol. **29**, 084007 (2014).

[6] J. R. Grandusky, S. R. Gibb, M. C. Mendrick, C. Moe, M. Wraback, and L. J. Schowalter, High output power from 260 nm pseudomorphic ultraviolet light-emitting diodes with improved thermal performance, Appl. Phys. Express **4**, 082101 (2011).

[7] T. Takano, T. Mino, J. Sakai, N. Noguchi, K. Tsubaki, and H. Hirayama, Deep-ultraviolet light-emitting diodes with external quantum efficiency higher than 20% at 275 nm achieved by improving light-extraction efficiency, Appl. Phys. Express **10**, 031002 (2017).

[8] R. Akaike, S. Ichikawa, M. Funato, and Y. Kawakami, $Al_xGa_{1-x}N$-based semipolar deep ultraviolet light-emitting diodes, Appl. Phys. Express **11**, 061001 (2018).

[9] M. Kneissl, T.-Y. Seong, J. Han, and H. Amano, The emergence and prospects of deep-ultraviolet light-emitting diode technologies, Nat. Photon. **13**, 233 (2019).

[10] H. Miyake, C.-H. Lin, K. Tokoro, and K. Hiramatsu, Preparation of high-quality AlN on sapphire by high-temperature face-to-face annealing, J. Crystal Growth **456**, 155 (2016).

[11] H. Yoshida, Y. Yamashita, M. Kuwabara, and H. Kan, Demonstration of an ultraviolet 336 nm AlGaN multiple-quantum-well laser diode, Appl. Phys. Lett. **93**, 241106 (2008).

[12] Z. Zhang, M. Kushimoto, T. Sakai, N. Sugiyama, L. Schowalter, C. Sasaoka, and H. Amano, A 271.8 nm deep-ultraviolet laser diode for room temperature operation, Appl. Phys. Express **12**, 124003 (2019).

[13] K. Sato, S. Yasue, K. Yamada, S. Tanaka, T. Omori, S. Ishizuka, S. Teramura, Y. Ogino, S. Iwayama, H. Miyake, M. Iwaya, T. Takeuchi, S. Kamiyama, and I. Akasaki, Room-temperature operation of AlGaN ultraviolet-B laser diode at 298 nm on lattice-relaxed $Al_0.6Ga_0.4N$/AlN/sapphire, Appl. Phys. Express **13**, 031004 (2020).

[14] Z. Zhang, M. Kushimoto, A. Yoshikawa, K. Aoto, L. J. Schowalter, C. Sasaoka, and H. Amano, Continuous-wave lasing of AlGaN-based ultraviolet laser diode at 274.8 nm by current injection, Appl. Phys. Express **15**, 041007 (2022).

[15] S.-H. Park and S.-L. Chuang, Crystal-orientation effects on the piezoelectric field and electronic properties of strained wurtzite semiconductors, Phys. Rev. B **59**, 4725 (1999).

[16] S. Ichikawa, Y. Iwata, M. Funato, S. Nagata, and Y. Kawakami, High quality semipolar $(1\bar{1}02)$ AlGaN/AlN quantum wells with remarkably enhanced optical transition probabilities, Appl. Phys. Lett. **104**, 252102 (2014).

[17] M. Suzuki, T. Uenoyama, and A. Yanase, First-principles calculations of effective-mass parameters of AlN and GaN, Phys. Rev. B **52**, 8132 (1995).

[18] S.-H. Wei and A. Zunger, Valence band splittings and band offsets of AlN, GaN, and InN, Appl. Phys. Lett. **69**, 2719 (1996).

[19] J. Li, K. B. Nam, M. L. Nakarmi, J. Y. Lin, H. X. Jiang, P. Carrier, and S.-H. Wei, Band structure and fundamental optical transitions in wurtzite AlN, Appl. Phys. Lett. **83**, 5163 (2003).

[20] E. Silveira, J. A. Freitas Jr., O. J. Glembocki, G. A. Slack, and L. J. Schowalter, Excitonic structure of bulk AlN from optical reflectivity and cathodoluminescence measurements, Phys. Rev. B **71**, 041201(R) (2005).

[21] G. Rossbach, M. Feneberg, M. Röppischer, C. Werner, N. Esser, C. Cobet, T. Meisch, K. Thonke, A. Dadger, J. Bläsing, A. Krost, and R. Goldhahn, Influence of exciton-phonon coupling and strain on the anisotropic optical response of wurtzite AlN around the band edge, Phys. Rev. B **83**, 195202 (2011).

[22] R. Ishii, A. Kaneta, M. Funato, and Y. Kawakami, Complete set of deformation potentials for AlN determined by reflectance spectroscopy under uniaxial stress, Phys. Rev. B **87**, 235201 (2013).

[23] P. P. Paskov, T. Paskova, P. O. Holtz, and B. Monemar, Polarized photoluminescence study of free and bound excitons in free-standing GaN, Phys. Rev. B **70**, 035210 (2004).

[24] K. Kojima, M. Ueda, M. Funato, and Y. Kawakami, Photoluminescence and optical reflectance investigation of semipolar and nonpolar GaN, Phys. Stat. Sol. (b) **244**, 1853 (2007).

[25] R. Ishii, A. Kaneta, M. Funato, Y. Kawakami, and A. A. Yamaguchi, All deformation potentials in GaN determined by reflectance spectroscopy under uniaxial stress: Definite breakdown of the quasicubic approximation, Phys. Rev. B **81**, 155202 (2010).

[26] R. G. Banal, M. Funato, and Y. Kawakami, Optical anisotropy in [0001]-oriented $Al_xGa_{1-x}N$/AlN quantum wells ($x > 0.69$), Phys. Rev. B **79**, 121308(R) (2009).

[27] J. E. Northrup, C. L. Chua, Z. Yang, T. Wunderer, M. Kneissl, N. M. Johnson, and T. Kolbe, Effect of strain and barrier composition on the polarization of light emission from AlGaN/AlN quantum wells, Appl. Phys. Lett. **100**, 021101 (2012).

[28] M. Guttmann, F. Mehnke, B. Belde, F. Woll, C. Reich, L. Sulmoni, T. Wernicke, and M. Kneissl, Optical light polarization and light extraction efficiency of AlGaN-based LEDs emitting between 264 and 220 nm, Jpn. J. Appl. Phys. **58**, SCCB20 (2019).

[29] M. Funato, K. Matsuda, R. G. Banal, R. Ishii, and Y. Kawakami, Strong optical polarization in nonpolar $(1\bar{1}00)$ $Al_xGa_{1-x}N$/AlN quantum wells, Phys. Rev. B **87**, 041306(R) (2013).

[30] R. Banal, Y. Taniyasu, and H. Yamamoto, Deep-ultraviolet light emission properties of nonpolar *M*-plane AlGaN quantum wells, Appl. Phys. Lett. **105**, 053104 (2014).

[31] K. Balakrishnan, V. Adivarahan, Q. Fareed, M. Lanhab, B. Zhang, and A. Khan, First demonstration of semipolar deep ultraviolet light emitting diode on *m*-plane sapphire with AlGaN multiple quantum wells, Jpn. J. Appl. Phys. **49**, 040206 (2010).

[32] K. Ueno, A. Kobayashi, J. Ohta, and H. Fujioka, Structural properties of semipolar $Al_xGa_{1-x}N$ $(1\bar{1}03)$ films grown on ZnO substrates using room temperature epitaxial buffer layers, Phys. Stat. Sol. (a) **207**, 2149 (2010).

[33] J. Stellmach, F. Mehnke, M. Frentrup, C. Reich, J. Schlegel, M. Pristovsek, T. Wernicke, and M. Kneissl, Structural and optical properties of semipolar $(11\bar{2}2)$ AlGaN grown on $(10\bar{1}0)$ sapphire by metal-organic vapor phase epitaxy, J. Crystal Growth **367**, 42 (2013).

[34] T. Wunderer, Z. Yang, M. Feneberg, M. Batres, M. Teepe, and N. Johnson, Structural and optical characterization of AlGaN multiple quantum wells grown on semipolar (20–21) bulk AlN substrate, Appl. Phys. Lett. **111**, 111101 (2017).

[35] M. Jo, Y. Itakazu, S. Kuwaba, and H. Hirayama, Controlled crystal orientations of semipolar AlN grown on an *m*-plane sapphire by MOCVD, Jpn. J. Appl. Phys. **58**, SC1031 (2019).

[36] S. Ichikawa, M. Funato, and Y. Kawakami, Metalorganic vapor phase epitaxy of pit-free AlN homoepitaxial films on various semipolar substrates, J. Crystal Growth **522**, 68 (2019).

[37] I. Vurgaftman and J. R. Meyer, Band parameters for nitrogen-containing semiconductors, J. Appl. Phys. **94**, 3675 (2003).

[38] T. Takano, Y. Narita, A. Horiuchi, and H. Kawanishi, Room-temperature deep-ultraviolet lasing at 241.5 nm of AlGaN multiple-quantum-well laser, Appl. Phys. Lett. **84**, 3567 (2004).

[39] M. Lachab, F. Asif, A. Coleman, I. Ahmad, B. Zhang, V. Adivarahan, and A. Khan, Optically-pumped 285 nm edge stimulated emission from AlGaN-based LED structures grown by MOCVD on sapphire substrates, Jpn. J. Appl. Phys. **53**, 112101 (2014).

[40] Y. Tian, Y. Zhang, J. Yan, X. Chen, J. Wang, and J. Li, Stimulated emission at 272 nm from an $Al_xGa_{1-x}N$-based multiple-quantum-well laser with two-step etched facets, RSC Adv. **6**, 50245 (2016).

[41] X.-H. Li, T. Detchprohm, T.-T. Kao, M. M. Satter, S.-C. Shen, P. D. Yoder, R. D. Dupuis, S. Wang, Y. O. Wei, H. Xie, A. M. Fischer, F. A. Ponce, T. Wernicke, C. Reich, M. Martens, and M. Kneissl, Low-threshold stimulated emission at 249 nm and 256 nm from AlGaN-based multiple-quantum-well lasers grown on sapphire substrates, Appl. Phys. Lett. **105**, 141106 (2014).

[42] V. N. Jmerik, E. V. Lutsenko, and S. V. Ivanov, Plasma-assisted molecular beam epitaxy of AlGaN heterostructures for deep-ultraviolet optically pumped lasers, Phys. Stat. Sol. (a) **210**, 439 (2013).

[43] E. V. Lutsenko, N. V. Rzheutskii, V. N. Pavlovskii, G. P. Yablonskii, D. V. Nechaev, A. A. Sitnikova, V. V. Ratnikov, Y. V. Kuznetsova, V. N. Zhmerik, and S. V. Ivanov, Spontaneous and stimulated emission in the mid-ultraviolet range of quantum-well heterostructures based on AlGaN compounds grown by molecular beam epitaxy on c-sapphire substrates, Phys. Solid State **55**, 2173 (2013).

[44] F. Asif, M. Lachab, A. Coleman, I. Ahmad, B. Zhang, V. Adivarahan, and A. Khan, Deep ultraviolet photopumped stimulated emission from partially relaxed AlGaN multiple quantum well heterostructures grown on sapphire substrates, J. Vac. Sci. Technol. B **32**, 061204 (2014).

[45] X.-H. Li, T.-T. Kao, M. M. Satter, Y. O. Wei, S. Wang, H. Xie, S.-C. Shen, P. D. Yoder, A. M. Fischer, F. A. Ponce, T. Detchprohm, and R. D. Dupuis, Demonstration of transverse-magnetic deep-ultraviolet stimulated emission from AlGaN multiple-quantum-well lasers grown on a sapphire substrate, Appl. Phys. Lett. **106**, 041115 (2015).

[46] J. Xie, S. Mita, Z. Bryan, W. Guo, L. Hussey, B. Moody, R. Schlesser, R. Kirste, M. Gerhold, R. Collazo, and Z. Sitar, Lasing and longitudinal cavity modes in photo-pumped deep ultraviolet AlGaN heterostructures, Appl. Phys. Lett. **102**, 171102 (2013).

[47] Y.-S. Liu, Z. Lochner, T.-T. Kao, M. M. Satter, X.-H. Li, J.-H. Ryou, S.-C. Shen, P. D. Yoder, T. Detchprohm, R. D. Dupuis, Y. Wei, H. Xie, A. Fischer, and F. Ponce, Optically pumped AlGaN quantum-well lasers at sub-250 nm grown by MOCVD on AlN substrates, Phys. Stat. Sol. (c) **11**, 258 (2014).

[48] Z. Lochner, T.-T. Kao, Y.-S. Liu, X.-H. Li, M. M. Satter, S.-C. Shen, P. D. Yoder, J.-H. Ryou, R. D. Dupuis, Y. Wei, H. Xie, A. Fischer, and F. A. Ponce, Deep-ultraviolet lasing at 243 nm from photo-pumped AlGaN/AlN heterostructure on AlN substrate, Appl. Phys. Lett. **102**, 101110 (2013).

[49] Z. Lochner, T.-T. Kao, Y.-S. Liu, X.-H. Li, M. M. Satter, S.-C. Shen, P. D. Yoder, J.-H. Ryou, R. D. Dupuis, Y. Wei, H. Xie, A. Fischer, and F. A. Ponce, Room-temperature optically pumped AlGaN-AlN multiple-quantum-well lasers operating at < 260 nm grown by metalorganic chemical vapor deposition, Proc. SPIE **8625**, 862519 (2013).

[50] T. Wunderer, C. L. Chua, Z. Yang, J. E. Northrup, N. M. Johnson, G. A. Garrett, H. Shen, and M. Wraback, Pseudomorphically grown ultraviolet C photopumped lasers on bulk AlN substrates, Appl. Phys. Express **4**, 092101 (2011).

[51] Z. Lochner, X.-H. Li, T.-T. Kao, M. M. Satter, H. J. Kim, S.-C. Shen, P. D. Yoder, J.-H. Ryou, R. D. Dupuis, K. Sun, Y. Wei, T. Li, A. Fischer, and F. A. Ponce, Stimulated emission at 257 nm from optically-pumped AlGaN/AlN heterostructure on AlN substrate, Phys. Stat. Sol. (a) **210**, 1768 (2013).

[52] M. Lachab, W. Sun, R. Jain, A. Dobrinsky, M. Gaevski, S. Rumyantsev, M. Shur, and M. Shatalov, Optical polarization control of photo-pumped stimulated emissions at 238 nm from AlGaN multiple-quantum-well laser structures on AlN substrates, Appl. Phys. Express **10**, 012702 (2017).

[53] T.-T. Kao, Y.-S. Liu, M. M. Satter, X.-H. Li, Z. Lochner, P. D. Yoder, T. Detchprohm, R. D. Dupuis, S.-C. Shen, J.-H. Ryou, A. M. Fischer, Y. Wei, H. Xie, and F. A. Ponce, Sub-250 nm low-threshold deep-ultraviolet AlGaN-based heterostructure laser employing HfO_2/SiO_2 dielectric mirrors, Appl. Phys. Lett. **103**, 211103 (2013).

[54] Y.-S. Liu, T.-T. Kao, M. M. Satter, Z. Lochner, X.-H. Li, S.-C. Shen, P. D. Yoder, T. Detchprohm, R. D. Dupuis, Y. Wei, H. Xie, A. Fischer, and F. A. Ponce, Optically-pumped deep-ultraviolet AlGaN multi-quantum-well lasers grown by metalorganic chemical vapor deposition, Proc. SPIE **9002**, 90020H (2014).